Star Clusters: From the Milky Way to the Early Universe
Proceedings IAU Symposium No. 351, 2019
A. Bragaglia, M. Davies, A. Sills & E. Vesperini, eds.

doi:10.1017/S1743921319007178

Chemical and kinematic study of Large Magellanic Cloud RGB stars

Alice Minelli[1,2] **and Alessio Mucciarelli**[1,2]

[1]Dipartimento di Fisica e Astronomia - Alma Mater Studiorum Università di Bologna
via Piero Gobetti 93/2, 40129 Bologna, Italy

[2]INAF - Osservatorio di Astrofisica e Scienza dello Spazio di Bologna
via Piero Gobetti 93/3, 40129 Bologna, Italy
emails: alice.minelli4@unibo.it, alessio.mucciarelli2@unibo.it

Abstract. The Large Magellanic Cloud (LMC) is the closest massive satellite of the Milky Way (MW), and its proximity allows us to study its stellar populations with great detail, both with resolved photometry and spectroscopy. In turn, this is crucial to unveil its star formation and chemical enrichment histories, and also to investigate the effects that gravitational interactions with other systems (as the Small Magellanic Cloud (SMC) and the MW) may induce on an irregular galaxy. The LMC is characterized by a still on-going star formation activity, as traced by the wide range of ages and metallicities of its stellar populations. However, most of the information about the chemistry and the kinematics of this galaxy has been obtained from low-resolution spectra, which do not allow to draw firm conclusions on many crucial open questions. In particular, (1) we still miss a homogeneous determination of the LMC metallicity distribution; (2) the metal-poor component is still poorly known and described; and (3) we have no conclusive information on the existence of metallicity gradients, which would suggest to spatially inhomegeneous star formation events. To properly address these issues, we analysed nearly 500 high-resolution FLAMES spectra of red giant stars belonging to the LMC field, the largest set of high- resolution spectra of LMC stars analysed so far in a homogeneous way.

Keywords. galaxies: irregular - Local Group, stars: abundances, stars: kinematics.

1. Analysed targets

The analysed targets are RGB stars belonging to the LMC, located near to the RGB-Tip, sampling the stellar populations older than 1 Gyr. The stars have been selected from SOFI and 2MASS photometic catalogs.

The selected stars are located in 6 different regions of the LMC, located around the same number of globular clusters. The chosen positions of fields were made to analyse different parts of the galaxy: 3 of them are located along the central bar and 3 in more external regions. Fig. 1 shows the positions of fields in the galaxy, and Table 1 lists the distance of each field from the LMC center (van der Marel & Cioni 2001).

2. Spectral analysis

The observations have been performed with the multi-object spectrograph FLAMES at VLT, using two high-resolution setups, namely HR11 (spectral range $\lambda = 559.7$-584.0 nm, resolution $R = 29500$) and HR13 ($\lambda = 612.0$-640.5 nm, $R = 26400$).

Atmospherical parameters: An accurate calculation of the atmospherical parameters of the analysed stars is necessary for the determination of their chemical abundances.

Table 1. Distances from the adopted center (van der Marel & Cioni 2001) for the six studied fields.

field	distance (deg)	distance (kpc)
F1	10.0	8.7
F	23.6	3.1
F3	1.3	1.1
F4	3.3	2.9
F5	4.5	3.9
F6	4.6	4.0

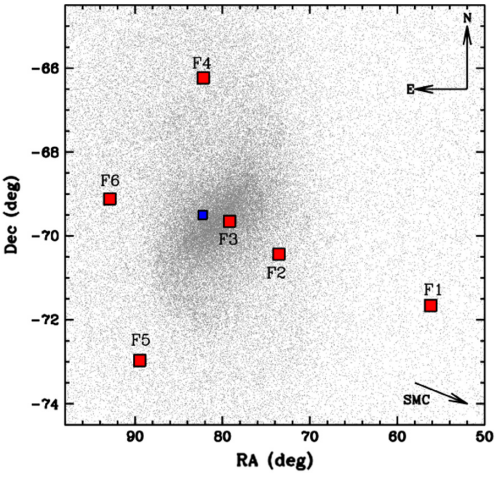

Figure 1. Spatial position of the observed fields (red squares). Blue square indicates the position of the LMC center by van der Marel & Cioni (2001).

- T_{eff} is determined from the IR flux method, using the relation between $(J-K)_0 - T_{eff}$ which is calibrated directly in the photometric system 2MASS (González Hernández & Bonifacio 2009);

- $log\ g$ is calculated from the surface gravity definition, using the bolometric correction of Buzzoni *et al.* (2010) and a distance modulus of 18.5;

- ξ is derived from Kirby relation which links the microturbolent velocity with $log\ g$. (Kirby *et al.* 2009)

Derived information: The information derived from the target spectra are:

- Radial Velocity (RV), measured from the Doppler shift of nearly 50 recognized unblended lines, using DAOSPEC (Stetson & Pancino 2008);

- $[Fe/H]$, determined from the Equivalent Width of the same lines with the GALA code (Mucciarelli *et al.* 2013).

3. Results

3.1. *Kinematics of the LMC*

The kinematic study of the LMC leads to two important results.

(1) The mean RV of each field changes with the position in the galaxy, as it is shown in Fig. 2. This variation is consistent with a rotational effect. This is the first evidence of rotation of the LMC disk derived using high-resolution spectra of intermediate-age/old giant stars.

(2) The velocity dispersion profile displays a constant behavior in the inner part of the LMC, with a possible external decrease (Fig. 3).

https://doi.org/10.1017/S1743921319007178 Published online by Cambridge University Press

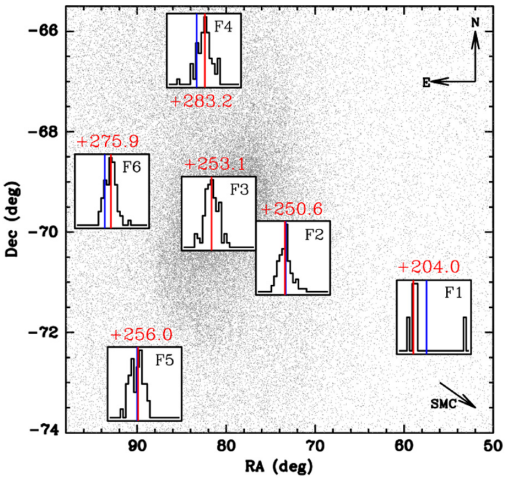

Figure 2. Spatial distribution of the observed fields with superimposed the corresponding RV distributions. For each histogram, the median value of the distribution is marked in red, instead the blue line is the median value of the central field.

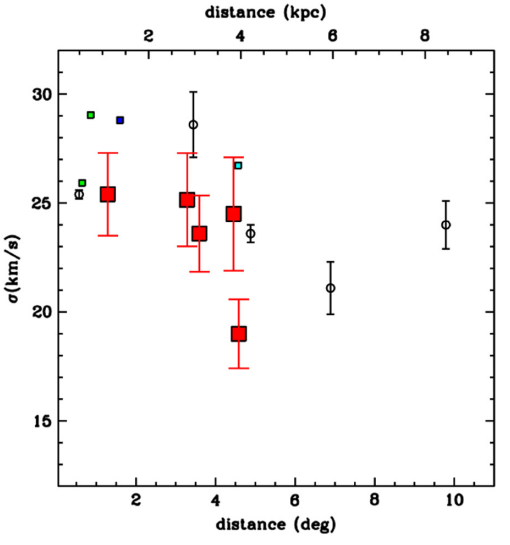

Figure 3. Velocity dispersion as a function of the distance from the LMC center. Squares are results from high-resolution studies: in red our work, in blue Pompéia *et al.* (2008), in cyan Lapenna *et al.* (2012), in green Song *et al.* (2017). Open circles: results from low-resolution studies (Carrera *et al.* 2011).

3.2. *Metallicity distribution of the LMC*

From the chemical analysis of the observed spectra we derive the iron abundance of each star.

In each field the metallicity distribution shows a different value of the peak. In particular, this value decreases moving outwards, and, in general, the northern region shows higher metallicities than the southern region. This is shown in Fig. 4 pointing out the presence of a metallicity gradient inside the galaxy.

https://doi.org/10.1017/S1743921319007178 Published online by Cambridge University Press

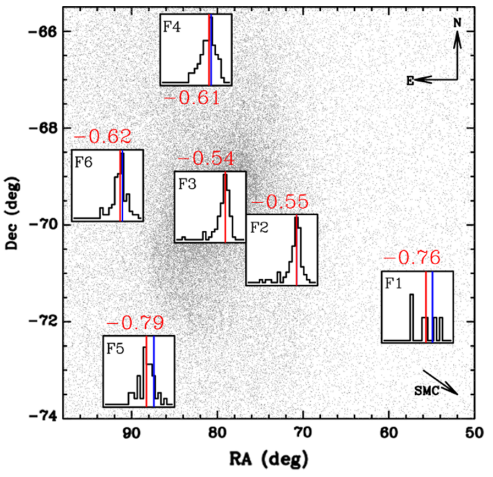

Figure 4. As Fig. 2, but with superimposed the metallicity distribution of each field.

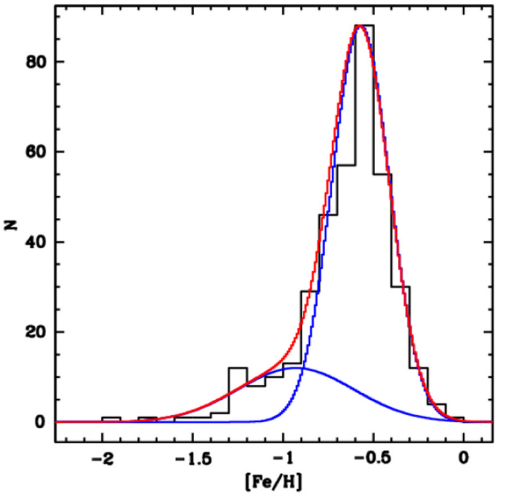

Figure 5. Total metallicity distribution of studied stars with superimposed the two identified Gaussian components.

The metallicity distributions of each field, excluding the most external one that is affected by low statistics, have some common characteristics: (1) the presence of a dominant component, with a peak around $[Fe/H] \sim -0.5$ dex; (2) the existence of a metal-poor component; (3) the lack of stars with metallicity lower than -2 dex or higher than the solar abundances. The total metallicity distribution of the six fields (Fig. 5) can be described as the sum of two different Gaussian components, where the dominant one is metal rich and with a metallicity dispersion smaller than the secondary metal-poor component. The distribution can be linked to the Star Formation History of the LMC provided by Harris & Zaritsky (2009): the metal-rich component is related to the star formation episode occurred 4–5 Gyr ago, following the tidal capture of the SMC from the LMC, that generates most of the stellar content of the galaxy, whereas, the metal-poor population (10% of the total) formed during the first burst of star formation (only 1% of the total, with $[Fe/H] < -1.5$ dex) and in the long period of quiescence between 13 and 5 Gyr ago.

https://doi.org/10.1017/S1743921319007178 Published online by Cambridge University Press

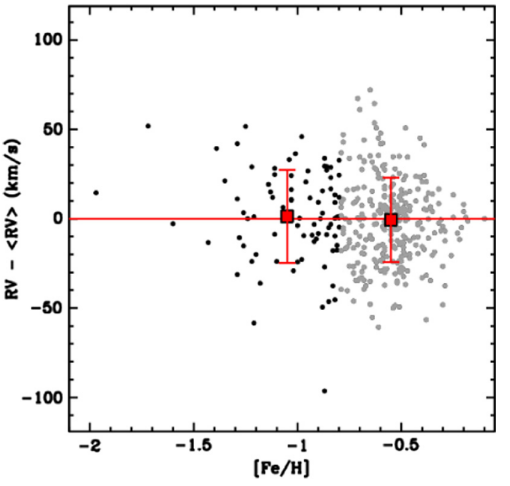

Figure 6. Behaviour of RV (shifted with respect to the peak of the RV distribution) of the individual stars as a function of $[Fe/H]$. Red squares indicate the median RV for the stars lower and higher than $[Fe/H] = -0.8$ dex and the errorbars are the corresponding velocity dispersions.

3.3. *Search for substructures*

Thanks to the information derived from the chemical and the kinematical study of the LMC, we search for stellar populations distinct in terms of metallicity and kinematics. No evidence of substructures is found, as it can be seen in the Fig. 6, where the total sample is divided in 2 groups adopting a cut of in metallicity at $[Fe/H] = -0.8$ dex. The derived velocity dispersions are compatible within the errors ($\sigma^{RV}_{metal-rich} = 23.6 \pm 1.0$ km/s, $\sigma^{RV}_{metal-poor} = 26.0 \pm 2.0$ km/s), therefore there is no evidence of the presence of a metal poor, kinematically hot halo.

References

Buzzoni, A., Patelli, L., Bellazzini, M., Pecci, F. F., & Oliva, E. 2010, *MNRAS*, 403, 1592
Carrera, R., Gallart, C., Aparicio, A., & Hardy, E. 2011, *AJ*, 142, 61
González Hernández, J. I. & Bonifacio, P. 2009, *A&A*, 497, 497
Harris, J. & Zaritsky, D. 2009, *AJ*, 138, 1243
Kirby, E. N., Guhathakurta, P., Bolte, M., Sneden, C., & Geha, M. C. 2009, *ApJ*, 705, 328
Lapenna, E., Mucciarelli, A., Origlia, L., & Ferraro, F. R. 2012, *ApJ*, 761, 33
Mucciarelli, A., Pancino, E., Lovisi, L., Ferraro, F. R., & Lapenna, E. 2013, *ApJ*, 766, 78
Pompéia, L. *et al.* 2008, *A&A*, 480, 379
Song, Y.-Y., Mateo, M., Walker, M. G., & Roederer, I. U. 2017, *AJ*, 153, 261
Stetson, P. B. & Pancino, E. 2008, *PASP*, 120, 1332
van der Marel, R. P. & Cioni, M.-R. L. 2001, *AJ*, 122, 1807

https://doi.org/10.1017/S1743921319007178 Published online by Cambridge University Press